ISSN-E: 2697-3650

Minerva Journal
Vol.3, Issue. 8, (pp. 8-19)

https://doi.org/10.47460/minerva.v3i8.60

Simulation of Combined Stresses and Stress Concentration Factor Effects on a Femur Cortical Bones

Alex J. Velez-Cruz
https://orcid.org/0000-0002-9289-5256
alvelez@pupr.edu
Polytechnic University of Puerto Rico
San Juan, Puerto Rico

Recibido(16/04/2022), Aceptado(15/05/2022)

Abstract—- The purposes of this article were to obtain mechanical properties of the dry femur cortical bone samples through a tensile load and stress concentration factor approach and to provide simulations to predict experimental behaviors based on manipulations of certain properties and parameters of the biomaterial. Since bone samples have characteristics and geometries, the development of a mathematical model was necessary to describe the combination of stresses interacting in the bone when a tension load is applied. The samples have average diameters and lengths of 0.5 and 2 inches respectively and were tested using a 10 kN Universal Tensile Machine to determine mechanical properties such as yield and ultimate stress, young module, fracture, among others. Several simulations were conducted to evaluate failure criteria like "Von Mises", "Tresca" and "Tsai-Wu". Finally, was concluded that 83% of the data obtained from the 22 samples observed in the "Stress-Strain" charts showed a directly proportional relationship.

Keywords: mechanical properties, stress-strain curve, stress concentration factor, failure criteria simulation

Simulación de los Efectos de Combinaciones de Esfuerzo y Factor de Concentración de Esfuerzo en Hueso Femoral Cortical

Resumen—Los propósitos de este artículo fueron obtener propiedades mecánicas de muestras secas en hueso fémur a través de fuerzas en tensión y del factor de concentración de esfuerzos y proveer simulaciones para predecir comportamientos experimentales basados en manipulaciones de ciertos parámetros y propiedades. Dado que las muestras tienen geometrías características, fue necesario desarrollar un modelo matemático para describir las combinaciones de esfuerzos que interaccionaban en el hueso cuando se aplica una carga de tensión. Las muestras tienen diámetros promedios y longitudes de 0.5 y 2 pulgadas respectivamente y fueron evaluadas utilizando una Maquina de Tensión Universal para determinar propiedades mecánicas como esfuerzos ultimo y de fluencia, módulo de elasticidad, entre otras. Varias simulaciones fueron ejecutadas para evaluar criterio de fallas tales como "Esfuerzo Von Mises", "Tresca" y "Tsai-Wu". Finalmente, se concluyó que 83% de los datos obtenidos de 22 muestras observadas en gráficas "Esfuerzo-Desplazamiento" mostraron una relación directamente proporcional.

Palabras clave: propiedades mecánicas, curva de esfuerzo y desplazamiento, factor de concentración de esfuerzo, simulación de criterio de falla

I.Introduction

The characterization of biomaterials is necessary to determine the mechanical, chemical, and electrical, among other interesting properties of the material [1]. The mechanical property is obtained from a mechanical destructive test, called the tensile test. Basically, it is when a pulling force or tension is applied to materials until it fails or breaks, providing information about the Yield Strength (σ_y), Ultimate Tensile Strength (σ_{ult}), Ductility (D), Young's modulus (E), and Poisson's ratio (ν) of the material [2] [3] [4].

Bone is composed of three different types of bones, cortical, trabecular (cancellous), and marrow bones. Cortical bone is dense and solid and surrounds the marrow space, whereas trabecular bone is composed of a honeycomb-like network of trabecular plates and rods interspersed in the bone marrow compartment [5]. Those bones are separated into two main elements, the cellular component, and an extracellular matrix. The matrix, which is responsible for the mechanical strength of the bone tissue, is formed by an organic and a mineral phase, but a liquid component is also present [6]. By weight, bone contains approximately 60% mineral, 10% water, and about 30% collagenous matrix. The mineral component influences the stiffness of the bone, whereas the collagen network contributes significantly to its fracture properties.

Typically, engineers consider three basic tasks when biomaterials are being evaluated. The first, understanding the properties of the materials (strength, fatigue, among others); second, the analysis of the response of the study material when is subject to external loads (Free Body Diagrams) and third; the determination of the weakest areas of the material (stress concentration factors) [7]. The intended research is oriented to obtain the stress-strain relation of dry canine cadaveric cortical bone samples using the stress concentration factor (K_{scf}) analysis.

The (K_{scf}) is the ratio of the highest stress (σ_{max}) to reference stress (σ_{ref}) of the gross cross-section. This experimental factor shall be considered as part of the engineering analysis on the stress-strain curve since the mechanical properties of the biomaterial can be affected directly. During this research will be seen a combination of the stresses interacting on bone samples when they are subject to axial loads. Based on the destructive tensile test and the stress concentration factor approach, it is expected to see normal, bending and shear stresses influencing the behavior of the stress-strain curve.

Therefore, the target of this research will be focused to perform a simulation through a Computer Aid Drafting (CAD) tool (CREO Parametric) with the intent to use a failure criterion (Von Miss Stress, Tresca, Tsai-Wu, etc.) to determine their critical values before a fracture occurs and to compare those values among them. Also, will serve to model the interaction of the principal stresses and the effect that those stresses have on the behavior of the stress-strain curve. The new stress-strain curve obtained from the simulation will be compared against the experimental curve obtained from the tensile tests. Finally, error calculations are documented to analyze, describe, and predict the accuracy and precision of the proposed model as well as how well is behaving.

II. DEVELOPMENT

A. Mechanical Properties of the Bone

The diverse forms and geometries of cortical and trabecular bones result in different mechanical properties. The mechanical properties of the bone vary according to species, size, age, among other characteristics and parameters. The mineral content in a bone shows little changes with increasing age, and this behavior is observed in its stiffness. In contrast, the energy absorbed (toughness) during the fracture of bone decreases significantly with increasing age, which contributes to an inverse proportional relationship. The mineral phase most likely imparts stiffness to the bone, whereas the collagen network contributes significantly to its fracture properties [6].

Cortical bone is an anisotropic material, meaning that its mechanical properties vary according to the direction of load. The strength and tensile/compressive moduli of cortical bone along the longitudinal direction are greater than those along the radial and circumferential directions. Nowadays, minor fluctuations in mechanical properties have been observed in the radial versus circumferential direction, recommending that cortical bone can be considered as a transversely isotropic material. When samples receive tension along the longitudinal direction, cortical bone shows a bilinear stress-strain response in which a distinct yield point separates a linearly elastic region and a region of linear hardening that ends abruptly at a fracture strain of less than 3. Cortical bone specimens loaded in the transverse direction fail in a more brittle manner compared with those loaded in the longitudinal direction [8].

B. Stress-Strain Curve

The following diagram has the intent to provide detailed background information regarding the behavior of the femur bone material when is subject to tension loads.

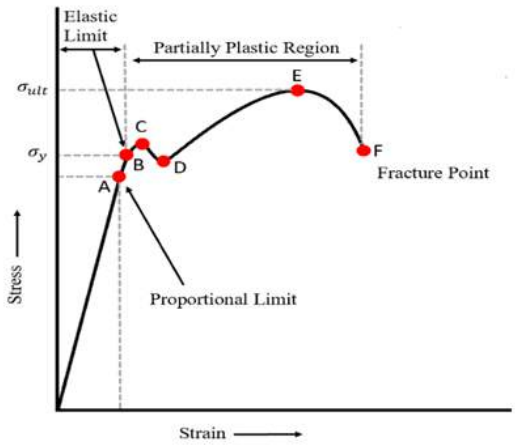

Fig. 1. Stress-Strain Diagram [9]

In Fig. 1 above, point A represents the proportional limit, which the slope of this line is better known as the Young's Modulus. For segment AB, the material may still be elastic in the sense that the deformations are completely recovered when the load is removed, and this point B is called the elastic limit or yield point. Point A and segment AB are part of the elastic region, which is governed by Hook's law. Beyond point B,

C. Principal Stresses

The engineering measures of stress (σ) and strain (ε) are determined from the measured load (P) and deflection (δ) using the original specimen cross-sectional area (A_0) and length (L_0) as:

$$\sigma = \frac{P}{A_0},\ \varepsilon = \frac{\delta}{L_0} \tag{1}$$

When the stress (σ) is plotted against the strain (ε), an engineering stress-strain curve such as that shown in Fig. 1 is obtained [10]. In the early phase of the stress-strain curve, various materials obey Hooke's law to a reasonable approximation, so that stress is proportional to strain with the constant of proportionality being the modulus of elasticity or Young's modulus (E) [11]:

$$\sigma = E \cdot \varepsilon \tag{2}$$

Since bones vary in geometry, a representation of the mathematical model is needed to explain the physical phenomena occurring during the experimental tests. Therefore, the following equation related to the combination of principal stresses (σt) (normal, bending, and shear) will be briefly discussed and further implemented in the proposed cortical bone model.

$$\sigma_t = k_{scf}(\sigma_n + \sigma_b + \tau) \tag{3}$$

The kscf, σn, σb and τ are provided as follows:

$$k_{scf} = \frac{\sigma_{max}}{\sigma_{ref}} \tag{4}$$

where stress concentration factor (kscf) is the ratio of the highest stress (σmax) to reference stress (σref) of the gross cross-section:

$$\sigma_n = \frac{F}{A} \tag{5}$$

where F is the applied normal force and A is the cross-sectional area of the specimen:

$$\sigma_b = \frac{F \cdot r}{I} \tag{6}$$

where F is the applied normal force, r is radio, and I is the inertia moment A is the cross-sectional area of the specimen:

$$\tau = \frac{3 \cdot V}{2 \cdot A} \tag{7}$$

and assuming a cylindrical hollow element, τ, can be approximated as described in (7), where V is the shear stress value and A is the cross-sectional area of the specimen. Thus, substituting (4), (5), (6) and (7) into (3), the final combined stresses equation is represented as follows:

$$\sigma_t = \frac{\sigma_{max}}{\sigma_{ref}}\left(\frac{F}{A} + \frac{F \cdot r}{I} + \frac{3 \cdot V}{2 \cdot A}\right) \tag{8}$$

D. Principal Strains

On the other hand, principal strains (maximum and minimum normal strains) shall be considered as part of the cortical bone behavior, which is obtained from differentiating axial (ε_x), and lateral (ε_y) with respect to θ. Then, the general equation for the total principal strains present in the experiment is provided as follows:

$$\varepsilon_t = \varepsilon_1 + \varepsilon_2 + \gamma_{xy} \tag{9}$$

where ε_1 and ε_2 are obtained from the following plane stress-strain formula [12]:

$$\varepsilon_{1,2} = \frac{\varepsilon_x + \varepsilon_y}{2} \pm \sqrt{\left(\frac{\varepsilon_x - \varepsilon_y}{2}\right)^2 + \left(\frac{\gamma_{xy}}{2}\right)^2} \tag{10}$$

where shear strain (γ_{xy}) is related with the orientation of the planes of the principal strains as follows:

$$\tan(2\theta) = \frac{\gamma_{xy}}{\varepsilon_x - \varepsilon_y} \tag{11}$$

According to the experiment provided there is no variation in the stress-strain planes, therefore, θ = 0, which makes $\gamma_{xy} = 0$ for all data collected from the experimental tests. Furthermore, no shear strains will be acting on the planes of the principal strains, which means that (10) will be eliminated from the principal stress analysis when simulation take place.

Nevertheless, substituting (9) into (8), the combined principal strains equation is represented as follow:

$$\varepsilon_t = \frac{\varepsilon_x + \varepsilon_y}{2} + \sqrt{\left(\frac{\varepsilon_x - \varepsilon_y}{2}\right)^2 + \left(\frac{\gamma_{xy}}{2}\right)^2} - \left(\frac{\varepsilon_x + \varepsilon_y}{2} + \sqrt{\left(\frac{\varepsilon_x - \varepsilon_y}{2}\right)^2 + \left(\frac{\gamma_{xy}}{2}\right)^2}\right) \tag{12}$$

Finally, incorporating (8) and (12) respectively (principal stresses and strains) into the mathematical model, predictions can be made through a simulation to determine the main objectives of this research, mechanical properties, and failure criteria.

E. Failure Criteria

Failure principles are used to determine and predict if a material will fail under certain circumstances, including loads, engineering parameters, mechanical properties, among others. From a mechanics of material perspective, exits basic failure criteria. For purpose of this research, the Distortion Energy (Von Mises), Tresca (Maximum Shear Stress) and Tsai-Wu (Failure Index) criteria will be used to evaluate the fracture point of the biomaterial. According to [13], Von Mises's theory, a ductile solid will yield when the distortion energy density reaches a critical value for that material. Since this should be true for the uniaxial stress state also, the critical value of the distortional energy can be estimated from the uniaxial test. Based on this experiment, the analysis is considered as two–dimensional plane stress state, which indicated that $\sigma_3 = 0$, simplifying the principal Von Mises stress equation as follows:

$$\sigma_{VM} = \sqrt{\sigma_1{}^2 - \sigma_1 \cdot \sigma_2 + \sigma_2{}^2} \tag{13}$$

For maximum shear stress theory, the material yields when the maximum shear stress at a point equals the critical shear stress value for that material. Since this should be true for uniaxial stress state, we can use the results from uniaxial tension test to determine the maximum allowable shear stress. The stress state in a tensile specimen at the point of yielding is given by: $\sigma_1 = \sigma_Y, \sigma_2 = \sigma_3 = 0$. The maximum shear stress is calculated as [13]:

$$\tau_{max} = \frac{\sigma_1 - \sigma_3}{2} \geq \tau_Y = \frac{\sigma_Y}{2} \qquad (14)$$

The Tsai-Wu failure criterion is one of the first failure criteria studied by scientists to evaluate factor of safety for composite materials. This failure criterion takes into consideration the total strain energy interacting in the specimen. Based on the experiment proposed, it can be assumed a bi-dimensional plane stress, which simplifies the equation to the following:

$$F_1\sigma_1 + F_2\sigma_2 + 2F_{12}\sigma_1\sigma_2 + F_{11}{\sigma_1}^2 + F_{22}{\sigma_2}^2 + F_6\tau_{12} + F_{66}{\tau_{12}}^2 = 1 \qquad (15)$$

A reasonable safety of factor (SOF) for engineering analysis should be greater than 1. The inverse of the SOF is failure index (Tsau-Wu), which means that Failure Index simulations with less than 1 are not going to fail.

III. METHODOLOGY

The bones are considered biological materials; therefore, health and safety must be present throughout the research to avoid and minimize any type of risk to researchers. The research conducted has a combination of methodologies since experimental tests, procedures, equipment protocols and observations were conducted with the intent to obtain representative real scenarios regarding the behavior of the bones when they critical axial loads are applied. In general terms, this research has focused in quantitative and experimental methodologies.

The canine cortical bone samples were collected by a veterinarian and temporarily stored in a freezer at 50 degrees Fahrenheit. The humerus and femur dry bone samples were extracted from adults and young dogs of mid and large sizes respectively. The samples were transported in a foam cooler covered with ice from the Veterinarian Hospital to the Bioimpedance Laboratory at the Polytechnic University of Puerto Rico. Then, samples were cleaned with water at room temperature (72 degrees Fahrenheit) to remove leftover tissues such as muscles, tendons, and ligaments. To preserve the dry samples in good shape were placed at the Bioimpedance Freezer at 50 degrees Fahrenheit and relative humidity of 55%.

This sample preparation of the cortical bones was divided into 4 different batches and each batch into 3 groups taking into consideration the following elements: type of bone, aging, and bone size, and including their associated parameters such as pin diameter, overall length, thickness, eccentricity, and external and internal diameter. The first group was identified with dry femur samples for adults' mid-size bones. Those samples were cut into two sections with lengths of two and one inches respectively. The samples two inches long were used for a destructive tensile test while the one inch was labeled and stored within the freezer to be used later for the Bioimpedance test. The final samples for this group have pin diameter, overall length, thickness, and external and internal diameter dimensions of 0.10, 2.0, 0.10, 0.20, 0.5, and 0.40 inches respectively. The second group was identified with dry humerus samples for adults' mid-size bones. Those samples were cut into two sections with lengths of two and one inches respectively. The samples two inches long were used for a destructive tensile test while the one inch was labeled and stored within the freezer to be used later for the Bioimpedance test. The final samples for this group have pin diameter, overall length, thickness, and external and internal diameter dimensions of 0.10, 2.0, 0.10, 0.20, 0.5, and 0.40 inches respectively.

The third group was identified with dry femur samples for adults' mid-size bones. Those samples were cut into two sections with lengths of two and one inches respectively. The samples two inches long were used for a destructive tensile test while the one inch was labeled and stored within the freezer to be used later for the Bioimpedance test. The final samples for this group have pin diameter, overall length, thickness, and external and internal diameter dimensions of 0.10, 1.5, 0.10, 0.20, 0.5, and 0.40 inches respectively. The fourth group was identified with dry femur samples for young large-size bones. Those samples were cut into two sections with lengths of two and one inches respectively. The samples two inches long were used for a destructive tensile test while the one inch was labeled and stored within the freezer to be used later for Bioimpedance tests. The final samples for this group have pin diameter, length, thickness, and external and internal diameter dimensions of 0.10, 3.0, 0.13, 0.25, 0.65, and 0.52 inches respectively.

The samples were cut and machined using a low-speed diamond saw. The diamond saw blade was immersed in a saline bath to minimize the heat created from friction, which has been shown to significantly affect the material properties, specifically, the plasticity of the cortical bone. Then, the sections cut from the humerus, and femur were placed in a bone chuck and a transverse cut was made along the axis of interest. Great care was taken when placing the bone sections in a bone chuck to ensure the axis of interest coincided with the axis of cutting. The cylindrical cortical bone samples were placed in a custom bone chuck, and a drill hole was made to remove the cancellous/trabecular bone from those samples. Also, additional cuts were made to level the uncut side and, if necessary, trim the ends to fit on the accessories manufactured, and customized for the universal tensile test machine since the existing and available grips are for metal specimens use only. Therefore, aluminum accessories (grips) were designed to minimize the crushing effect on the bone ends when a tension load is applied. Once the grips were manufactured according to technical specifications, the initial calibration and setup were done properly as presented in Fig. 2 below.

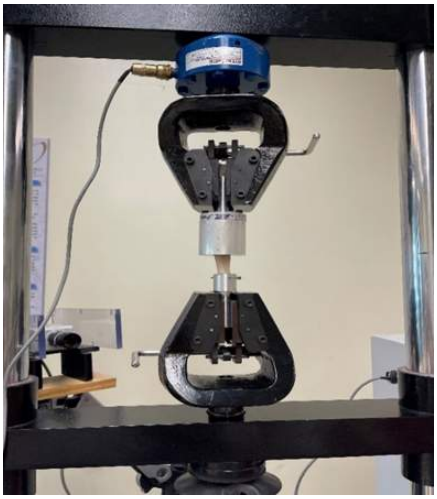

Fig. 2.Tensile Test Calibration and Setup

Prior to conducting the destructive tests, familiarization and practice with the tensile test machine and its software were required [14]. Also, safety, biohazard and waste disposal, and biomaterials handling trainings were taken to comply with US federal codes, standards, and regulations. The universal tensile machine used to perform the test was a brand Applied Test Systems, model 910, a double-column and rated at 10 kN. The machine pre-set values for pre-load cell, velocity and displacement were 100 lbs, 0.15 in/min, and 0.05 inches respectively.

IV. RESULTS

The experimental tests of the dry cortical bones were divided into two different types of charts, the first one "Load vs Displacement" and the other "Stress vs Strain". The Fig. 3 (a) represent the rough data obtained from the tensile tests while Fig. 3 (b) represents the relations between principal stresses and strains, including the stress concentration factor coefficient. The comparisons made between figures 3, 5 and 7 are necessary to determine the variations between rough data and math models, considering the load and displacement and principal stresses and strains parameters. The ultimate strength values from "batch 1, samples" obtained from figures 3 (b), 4 (b) and 5(b) are 11 (1,595), 39 (5,656) and 27 (3,916) MPa (Psi) respectively. The principal strains values on figures 3 (b), 4 (b) and 5(b) were obtained from ultimate strength points such as 0.0011, 0.0062 and 0.0023 respectively. Also, it has been noticed that beyond these ultimate strength values, the fracture process begins. The Young's modulus for 3 (b), 4 (b) and 5(b) were obtained as follows: 10 (1,450), 6,290 (912,287) and 11,739 (1,702,598) MPa (Psi). The charts provided in figures 3 (b), 4 (b) and 5(b) show a directly proportional relationship among the samples.

A statistics analysis was performed through Minitab for all samples presented in this article to evaluate the standard deviations, normal distribution, among other parameters. For descriptive analysis, it was assumed confidence level and error (α) of 95% and 5% respectively. The total "Load" data analyzed for batch 1-sample 1 was 39 readings and their mean, standard deviation and variance were 0.03819, 0.02280 and 0.00052 respectively. The histogram of this sample provided in Fig. 9 showed a normal distribution pattern. The 22 samples were analyzed and have been observed that other 21 samples showed similar trend to the one observed in Fig. 9.

The Fig. 6 shows the fracture detail in the samples. It was demonstrated that samples failed due to stress concentration factor with a combination of longitudinal and oblique fracture effects. The presence of normal and bending stresses along the samples validate that mathematical model serve to describe the physical phenomena encounter in the experimental tests. On Fig 7, the oblique fractures predominate against the longitudinal, indicating that more presence of bending was affecting the samples. Subsequently, it has been noticed that samples with non-uniform geometries played a big role in the engineering analysis.

In order to calibrate the model in CREO Parametric, the software request the entry of certain parameters and material properties such as Young's modulus, Poisson's ratio, yield strength and shear stiffness, which according to [12] were initially assumed as 6.964 x 108 psi, 0.4, 4,352 psi and 2.487 x 108 psi respectively: Based on experimental fracture points, which are the same than ultimate tensile strength value obtained from Fig. 3 (b), 4 (b) and 5(b) (1,595; 5,656 and 3,916 Psi respectively), and CREO simulation values obtained from Fig. 8 (a), which indicated a Von Mises stress value of 4,770.94 Psi, a comparison was made between Fig. 4 (b) and 8 (a) to determine the percentage of error between the model and the physical experiment. The corresponding percent of error was 15.64%. Since there is no validated standard or average values to works with canine cortical bones and the initial values used in CREO are slightly higher because corresponded to human cortical bones, the percent of error might be affected.

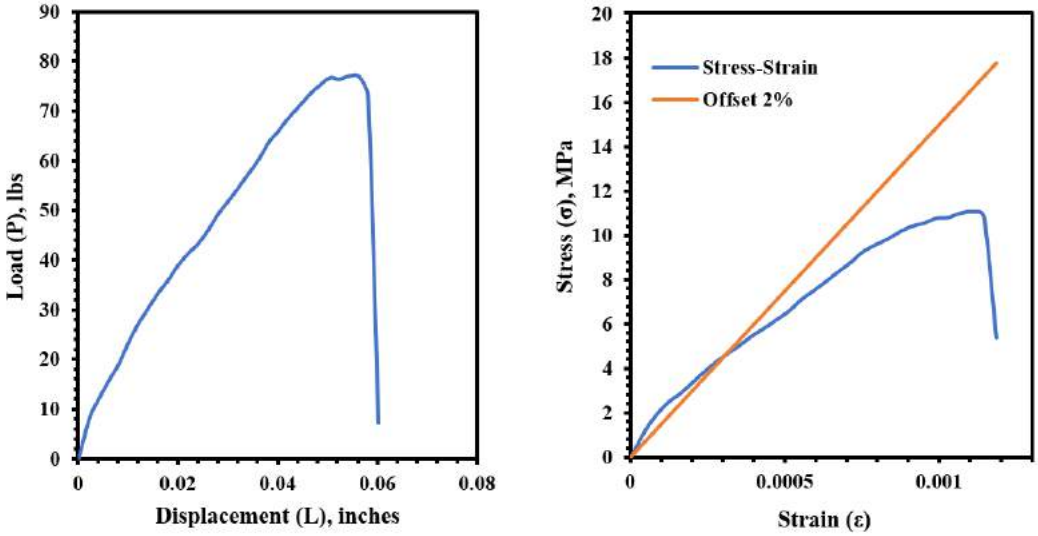

Fig. 3. (a) Load vs. Displacement (Batch 1, Sample 1)
(b) Principal Stress vs. Strain (Batch 1, Sample 1)

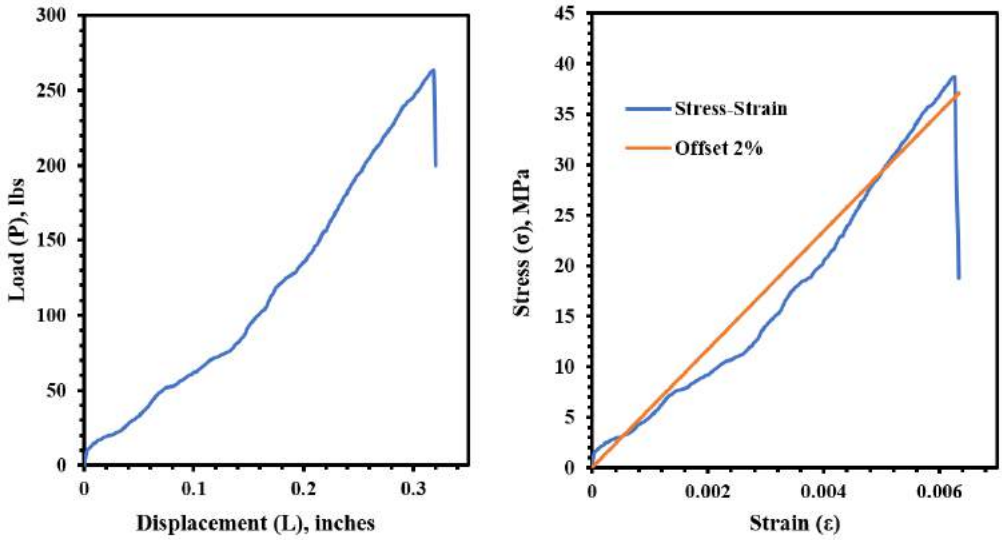

Fig. 4. (a) Load vs. Displacement (Batch 1, Samples 2 & 3) (b) Principal Stress vs. Strain (Batch 1, Samples 2 & 3)

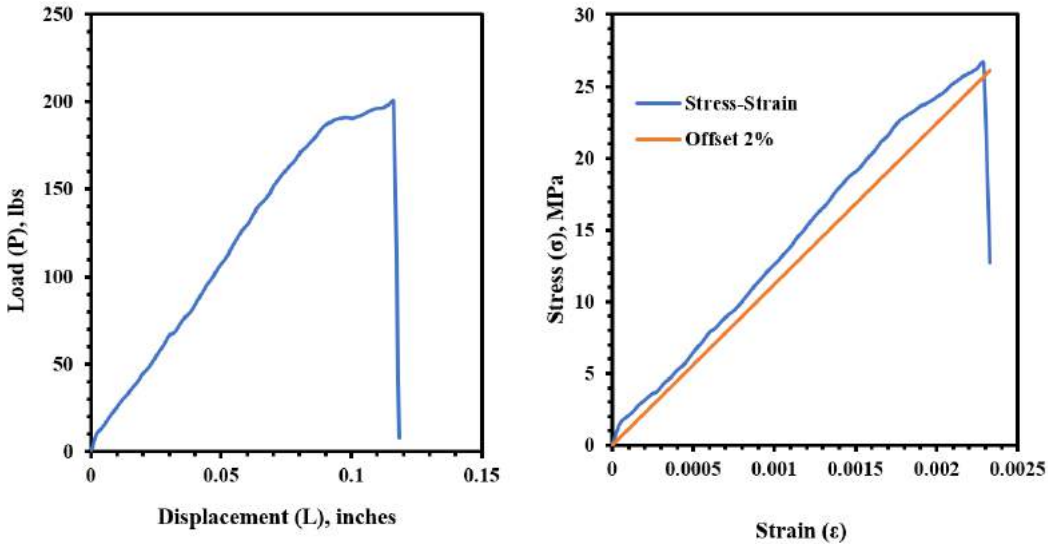

Fig. 5. (a) Load vs. Displacement (Batch 1, Samples 4 & 5) (b) Principal Stress vs. Strain (Batch 1, Samples 4 & 5)

Fig. 6 (a) Longitudinal Fracture on Batch 3, Sample 1 (b) Longitudinal Fracture on Batch 3, Sample 2 (c) Longitudinal Fracture on Batch 3, Sample 3

Fig. 7. Tensile Tests Results (a) Close View of the Oblique Fracture on Batch 1, Sample 1 (b) Oblique Fracture on Batch 3, Sample 1 (c) Oblique Fracture on Batch 3, Sample 4

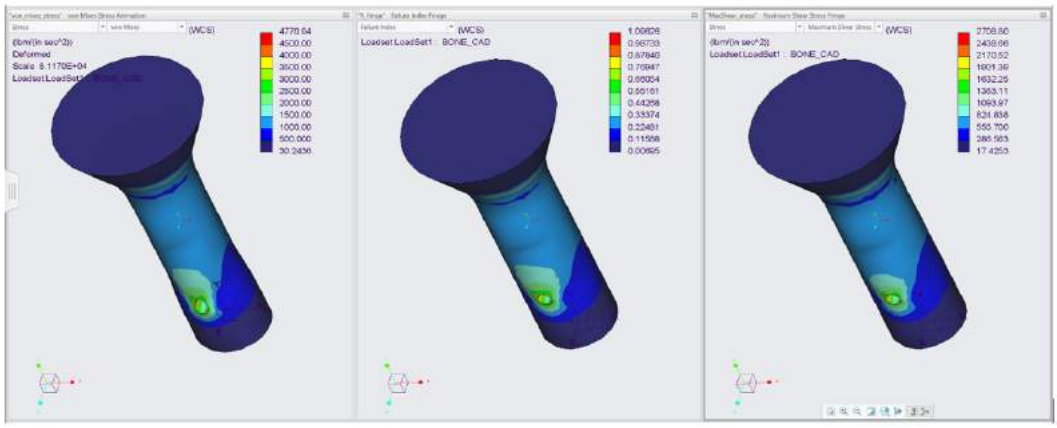

Fig. 8. Failure Criteria Simulation: (a) Von Mises Stress; (b) Failure Index; (c) Maximum Shear Stress

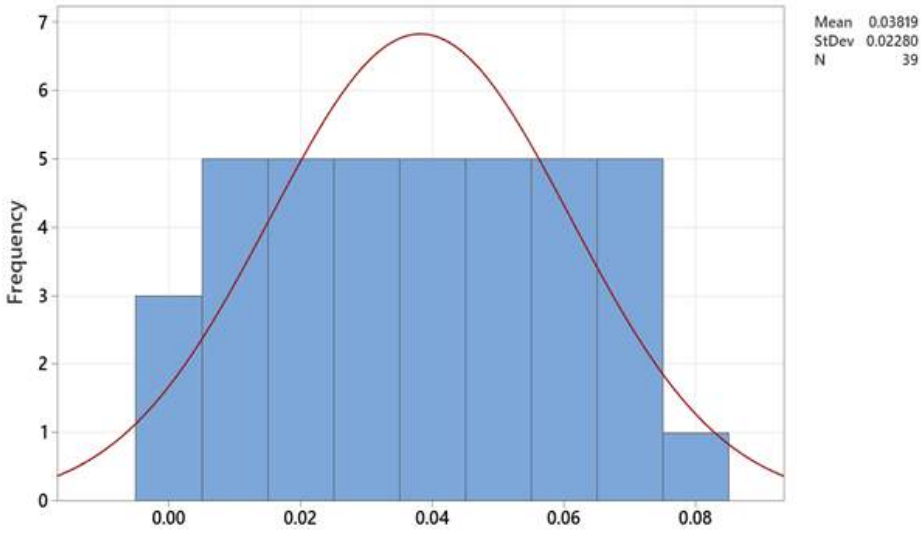

Fig. 9. Histogram of the Load-(Batch 1-Sample 1)

CONCLUSIONS

A comprehensive methodology for destructive mechanical tests were established for preparing and testing canine cadaveric cortical femur bone samples when are subject to axial loads and stress concentration factors to obtain mechanical properties of the biomaterial. It was concluded that 83% of the data obtained from the 22 samples observed from "Stress-Strain" charts showed a directly proportional relationship. The ultimate tensile strength (σult) values of the dry cortical femoral bones are equal to yield strength (σy) values, implying that bones samples behaved as a brittle material. Due to the small anisotropy of bone material analyzed (2 in length x 0.5 in diameter) the eccentricity distance was relatively small, that might influence the conclusions of the study. The standard deviations per batches were considered within acceptable parameters. The experimental results on cortical bones are closer to the predictions made by the simulation to evaluate failure criteria, considering a percentage of error of 15.64 %.

ACKNOWLEDGEMENT

I want to thank Dr. Luis Thomas Ramos from “San Francisco de Asis” Veterinarian Hospital to support this research by providing the femur and humerus bone samples. Also, I want to thank Dr. Julio Noriega Motta, Mechanical Engineering Department Head of the Polytechnic University of Puerto Rico to support with the mechanical tensile machine and manufacturing engineering laboratories.

REFERENCES

[1] A. Bandyopadhyay and S. Bose, Characterization of Biomaterials, Waltham, MA: Elsevier, 2013.
[2] J. Pelleg, Mechanical Properties of Materials, New York, London: Springer, 2013.
[3] M. Jaffe, W. B. Hammond, P. Tolias and A. Treena, Characterization of Biomaterials, Newark, NJ: Woodhead Publishing, 2012.
[4] G. R. Cointry, R. F. N. A. L. Capozza, E. J. Roldan and J. L. Ferretti, "Biomechanical Background for a Noninvasive Assessment of Bone Strength and Muscle-Bone Interactions," Journal Musculoskeletal Neuron Interact, vol. 4, no. 1, p. 1–11, 2003.
[5] B. Clarke, "Normal Bone Anatomy and Physiology," Clinical Journal of the American Society of Nephrology, vol. 3, no. 3, pp. 131-139, 2008.
[6] M. Basharat, A. Ikhlas and J. Azher, "Study of Mechanical Properties of Bones and Mechanics of Bone Fracture," in Proceedings of 60th Congress of ISTAM, Rajasthan, India, 2015.
[7] W. D. Pilkey, D. F. Pilkey and B. Zhuming, Peterson's Stress Concentration Factors, Hoboken, NJ: John Wiley & Sons, 2020.
[8] E. F. Morgan, G. U. Unnikrisnan and A. I. Hussein, "Bone Mechanical Properties in Healthy and Diseased States," Annu Rev Biomed Eng, vol. 20, no. 1, pp. 119-143, 2018.
[9] A. J. Velez-Cruz, Stress-Strain Diagram, Bayamon, PR: AVC Press, 2022.
[10] D.-3. ASTM Standard, Standard Test Methods for Composite Materials, West Conshohocken, PA: ASTM Press, 2004.
[11] D. Roylance, Stress-Strain Curves, Cambridge, MA: Cambridge MIT Press, 2001.
[12] B. Yang, Stress, Strain and Structural Dynamics, Los Angeles, CA: Academic Press , 2005.
[13] T. L. Anderson, Fracture Mechanics – Fundamentals and Applications, Boca de Raton, FL: CRC Press, 2006.
[14] ASTM Standard, E-8M-01, Standard Test Methods for Tensile Testing of Metallic Materials, West Conshohocken, PA: ASTM Press, 2004.